Smart utilization of cobalt-based double perovskite cathodes on barrier-layer-free zirconia electrolyte of solid oxide fuel cells

Meng Li[a,b], Kongfa Chen[b], Bin Hua[c], Jing-li Luo[c], William D.A. Rickard[d], Jian Li[a,*], John T.S. Irvine[e] and San Ping Jiang[b,*]

[*]Corresponding authors

[a]Center for Fuel Cell Innovation, State Key Laboratory for Coal Combustion, School of Materials Science and Engineering, Huazhong University of Science and Technology, Wuhan, Hubei 430074, China. Tel.: +86 27 87557694; fax: +86 27 87558142. E-mail address: lijian@hust.edu.cn.

[b]Fuels and Energy Technology Institute & Department of Chemical Engineering, Curtin University, Perth, WA 6102, Australia. E-mail address: s.jiang@curtin.edu.au.

[c]Department of Chemical and Materials Engineering, University of Alberta, Edmonton, Alberta T6G 2G6, Canada.

[d]John De Laeter Centre & Department of Physics and Astronomy, Curtin University, Perth, WA 6102, Australia.

[e]School of Chemistry, University of St Andrews, Fife KY16 9ST, UK.

Abstract

Cobaltite-based double perovskite oxides with high electrocatalytic activity and conductivity have been developed as high-performance cathode alternatives for solid oxide fuel cells (SOFCs). However, the use of cobaltite-based double perovskites on Y_2O_3 stabilized ZrO_2 (YSZ)-based SOFCs requires the application of a doped ceria barrier layer. This is due to their poor chemical and physical compatibility with YSZ electrolyte during high-temperature sintering and fabrication process. Here we report a viable approach of *in operando* assemble double perovskites such as $PrBa_{0.5}Sr_{0.5}Co_{1.5}Fe_{0.5}O_{5+\delta}$ (PBSCF) on YSZ electrolyte and thus effectively form an electrode/electrolyte interface without high temperature processing. The electrochemical performance of the *in situ* assembled PBSCF cathode is comparable to that of the cathode prepared by the conventional method. A single cell with an *in situ* assembled PBSCF-GDC (Gd-doped ceria) cathode achieved a peak power density (PPD) of 1.37 W cm^{-2} at 750 °C and exhibited a high stability at 500 mA cm^{-2} and 750 °C for 100 h. Surface and cross-sectional microstructure analysis offer solid evidence that the PBSCF-GDC cathode/YSZ electrolyte interface was formed by electrochemical polarization. This work offers new opportunities to effectively and effortlessly use high-performance double perovskite cathodes in commercial SOFCs.

1 Introduction

Solid oxide fuel cells (SOFCs) are great prospects for efficient and environmentally friendly energy conversion. Although their high operating temperature contributes to a high reaction rate, it also accelerates the degradations of both the cell and stack components. In this context, increasing efforts have been devoted to reducing the operating temperature to intermediate temperatures (500~800 °C). It has been found that the high cathodic overpotential loss becomes the key factor which undermines the performances of the SOFCs operating at reduced temperatures.[1-3] Thus, in order to improve the kinetics of the oxygen reduction reaction of SOFCs, considerable efforts have been made in the development of new cathodic materials with high activity and stability.

Recently, single-phase cobaltite-based perovskite materials, such as $LnBaCo_2O_{5+\delta}$ (Ln=Y, Gd, Sm, Nd, Pr) have been the subject of growing research activity for the ORR. Typically, they show a cation-ordered structure with alternating Ln-O and Ba-O layers.[4-6] Through proper ion substitution on both A and B sites, their physicochemical properties, such as electrical conductivities, electrochemical performances and redox stability could be effectively improved. For instance, $PrBa_{0.5}Sr_{0.5}Co_{1.5}Fe_{0.5}O_{5+\delta}$ (PBSCF) [7-9] showed the best electrochemical performance with very low area specific resistance (ASR) for oxygen reduction reaction (ORR), ~0.33 Ω cm^2 at 500 °C and ~0.056 Ω cm^2 at 600 °C. A Ni-GDC|GDC|PBSCF-GDC test cell demonstrated peak power density of ~2.16 W cm^{-2} at 600 °C and stable power output at 550 °C for 150 h under a cell voltage of 0.6 V. Unfortunately, the

practical application of these promising double perovskite materials is restrained due to their poor physicochemical compatibility with the state-of-art yttria-stabilized zirconia (YSZ) electrolyte. Double perovskites readily react with YSZ electrolyte during the high temperature sintering and fabrication process. In addition, the thermal expansion coefficients are vastly different from that of YSZ. Generated thermal stress at high temperatures may lead to detachment of cathode layer. A GDC buffer layer is generally adopted to prevent interactions between cathode and YSZ electrolyte layers, notwithstanding the TEC mismatch issue remains. The doped ceria buffer layer needs to be dense and pinhole-free and requires the careful control of the microstructure of the barrier layer and additional fabrication and sintering steps. In the case of metal-supported SOFCs cathodes cannot be sintered in an oxidizing atmosphere at above 1000 °C due to the deformation of the metal-support as a result of oxidation at high temperatures.[10-13] Thus, in order to use cobaltite-based cathodes such as $Ba_{0.5}Sr_{0.5}Co_{0.8}Fe_{0.2}O_{3-\delta}$ (BSCF) and $SmBa_{0.5}Sr_{0.5}Co_2O_{5+\delta}$ (SBSC) double perovskites on a ferritic stainless steel (STS430) supported full cell, GDC buffer layer was used without pre-sintering to prevent possible chemical reactions between YSZ electrolyte and cathode materials cathode layer.[10, 11] However, surface segregated Sr could migrate through the porous ceria barrier layer, forming insulating phase at the interface.

Most recently, we studied thermally and electrochemically induced electrode/electrolyte interfaces on pre-sintered and *in situ* assembled LSM and LSCF electrodes on YSZ and GDC electrolytes and found that electrode/electrolyte

interfaces can be formed on the *in situ* assembled cathodes under cathodic polarization conditions without the high temperature sintering process.[14] Although the topography of the electrochemically induced interface is very different from that of one formed under the conventional high temperature sintering, their electrocatalytic activities for the oxygen reduction reaction are close and comparable. In this study, the PBSCF and PBSCF-GDC cathodes were directly applied on anode-supported YSZ electrolyte based cells via *in situ* assembly method. The electrochemically induced cathode/YSZ electrolyte interfaces were formed by polarization at 500 mA cm^{-2} and 750 °C for 2 h and showed high activity and stability under SOFC operation conditions.

2 Experimental

2.1 Materials

$PrBa_{0.5}Sr_{0.5}Co_{1.5}Fe_{0.5}O_{5+\delta}$ (PBSCF) double perovskite was used as cathode material. To prepare PBSCF powder, $Pr(NO_3)_3{\cdot}6H_2O$ (Aldrich Chemistry), $Ba(NO_3)_2$ (Scharlau), $Sr(NO_3)_2$ (Chem-Supply), $Co(NO_3)_2{\cdot}6H_2O$ (Sigma-Aldrich) and $Fe(NO_3)_3{\cdot}9H_2O$ (Sigma-Aldrich) were initially dissolved in distilled water. Ethylene glycol and citric acid were added into the solution sequentially as the chelant agents. The molar ration of total metal ions, ethylene glycol and citric acid was 1:1.5:3. The solution was stirred and heated at 80 °C for 2 h, and then vaporized in an oven at 150 °C, followed by calcination in air at 1050 °C for 10 h to form layered perovskite PBSCF.

2.2 Cell fabrication

The anode-supported full cells (ϕ13 mm×1 mm) were prepared by tape-casting, screen printing and co-sintering process. The anode support substrate containing NiO (Inco) and 8 mol. % Y_2O_3 stabilized ZrO_2 (8YSZ, Tosoh) at a weight ratio of 57:43 was obtained by tape-casting. The NiO-YSZ (60:40) functional anode and YSZ electrolyte slurry were screen printed on one side of the anode support substrate in sequence, before sintered in air at 1390 °C for 3 h. To fabricate the PBSCF on YSZ electrolyte layer via conventional method, a GDC ($Ce_{0.9}Gd_{0.1}O_{1.95}$, AGC Semi Chemical CO., Ltd) buffer layer was fabricated on the YSZ electrolyte layer by spin coating and sintering at 1300 °C for 10 h. PBSCF cathode layer was then applied to the GDC buffer layer, followed by sintering at 950 °C in air for 4 h. In the case of *in situ* assembled PBSCF cathode, the cathode layer was painted directly on the YSZ electrolyte layer and dried at 100 °C for 1 h with no additional pre-sintering step at high temperatures. *In situ* assembled PBSCF-GDC (60:40) cathodes were prepared in similar way. The cathode area was 0.32 cm^2. Pt paste (Sino-Platinum Metals Co., Ltd) used as current collector was painted on the anode and cathode of as-prepared cells and dried at 100 °C for 1 h.

2.3 Characterization

The phase formation of as-prepared cathode powders was identified by X-ray diffraction (XRD). A thermal dilatometer (Linseis, L75 Platinum series) was used to examine the thermal expansion coefficient (TEC) of dense PBSCF sample in air from 200 to 900 °C.

Electrochemical polarization and impedance measurements were conducted by a

four probe method using a Zahner electrochemical workstation. Pt mesh and wires (Sino-Platinum Metals Co., Ltd) were used as current collector and measuring probes. The cells were sealed onto a cell holder (Al_2O_3 tube) by using a Ceramabond® glass sealant (Aremco Product, Inc.) and the NiO-YSZ anode was reduced by passing pure H_2 while being heated up. The cathodes were sintered *in situ* during heating up the cell to 750 °C, and then polarized at current density of 500 mA cm^{-2} for 2 h. After initial polarization, the electrochemical impedance spectra (EIS) and current density-voltage-power density (I-V-P) curves were measured at temperatures ranging from 650 to 750 °C. The stability of full cells with in situ assembled PBSCF-GDC cathode was evaluated at 750 °C by applying constant current and simultaneously keeping tracking of the voltage. Both H_2 and air were fed at a constant rate of 100 mL min^{-1} as fuel and oxidant, respectively, for all tests.

The microstructure of the cell with the composite cathode was examined by scanning electron microscope (SEM, Neon 40EsB) after polarization treatment. The topography at the cathode/electrolyte interface before and after polarization treatments was investigated using atomic force microscopy (AFM, Bruker's Dimension FastScan) with tapping mode and time-of-flight secondary ion mass spectrometry (TOF-SIMS, Lyra FIB-SEM). To investigate the cathode/electrolyte interface, the cathode layer was removed by immersing in HCl solution and ultrasonic bath for 15 min. Then the samples were left in the HCl for 24 h before cleaned thoroughly with distilled water.

3 Results and discussion

3.1 Phase and morphology characterization

Fig. 1 shows XRD and TEC results of synthesized PBSCF. The XRD pattern of as-prepared PBSCF powder is shown in Fig. 1a. The pattern shows only peaks associated with double perovskite structure without any evidence of the existence of any other impurities, according to JCPDS cards 00-053-0131 of $PrBaCo_2O_{5.68}$. This indicates that the as-synthesized PBSCF powder is pure double perovskite phase. The thermal expansion curve of PBSCF is not exactly linearly dependent on temperature, with an inflection occurring on the slope around 650 °C (Fig. 1b). The TEC value is 15.2×10^{-6} K^{-1} from 200 to 650 °C, and it increases to 31.5×10^{-6} K^{-1} at temperatures ranging from 650 to 900 °C. The reported TEC values are in the range of 10.3 to 10.7×10^{-6} K^{-1} for YSZ electrolyte.[15-17] The TEC value of PBSCF is much higher than that of the YSZ electrolyte. Nevertheless, the thermal mismatch between the YSZ electrolyte and double perovskite electrode could be accommodated by the loose and non-rigid microstructure of the *in situ* assembled electrode due to the absence of the high temperature sintering process.

3.2 Performance with *in situ* assembled pristine and composite cathodes

It is essential to compare performance difference of two full cells with PBSCF cathodes prepared by *in situ* assembling method and conventional method, respectively. Fig. 2a shows the polarization performance of cell with *in situ* assembled PBSCF cathode measured at 750 °C with H_2 as fuel and air as oxidant. The initial peak power density (PPD) is 0.48 W cm^{-2}. After a polarization current density of 500 mA cm^{-2} was applied to the cell for 2 h, the PPD is 0.54 W cm^{-2} at 750 °C, an 12.5%

increase as compared to that before polarization treatment. The results indicate that the polarization current passage improves the performance of the cells with *in situ* assembled PBSCF cathode. The promotion effect of polarization treatment on the cell performance is also confirmed by the impedance responses, as shown in Fig. 3b. The initial overall cell polarization and ohmic resistances (R_p and R_Ω) are 0.95 and 0.25 Ω cm^2, respectively, and decrease to 0.65 and 0.23 Ω cm^2 after polarization. In the case of the cell with pre-sintered PBSCF cathode, the PPD is 0.62 W cm^{-2} under the same conditions (Fig. 3a), slightly higher than that of the cell with *in situ* assembled PBSCF cathode. The cell with pre-sintered PBSCF cathode has similar ohmic resistance with that of the cell with *in situ* assembled PBSCF cathode, while its higher performance results from its lower R_p, 0.44 Ω cm^2. The close polarization performance of cells with *in situ* assembled and pre-sintered PBSCF cathodes indicates the feasibility of the in situ assembly method in the development of cobaltite-based double perovskite cathodes on YSZ electrolyte cells. As the R_p is strongly related to contact between PBSCF particles and the interfaces, optimization of the cathodic current treatment could further reduce R_p.

Figure 3 shows the electrochemical performance of the cell with an *in situ* assembled PBSCF-GDC composite cathode. The initial peak power density before polarization treatment is 1.11 W cm^{-2} (Fig. 3a), much higher than that of the cell with the *in situ* assembled pristine PBSCF cathode. After polarization treatment at 500 mA cm^{-2} and 750 °C for 2 h, the peak power density increases to 1.37 W cm^{-2}. The increase in power output is 23.4%, also higher than 12.5% performance improvement

experienced by the cell with pristine PBSCF cathode. The power density is 0.88 and 0.49 W cm^{-2} at 700 and 650 °C, respectively. The impedance behavior is similar to the polarization performance. Similar to the cell with pristine PBSCF cathode, both R_Ω and R_p of the cell with PBSCF-GDC composite cathode decrease after the polarization treatment (Fig. 4b). The R_Ω decreased from 0.24 to 0.20 Ω cm^2 whilst the R_p decreased from 0.52 to 0.32 Ω cm^2 at 750 °C. The decrease in polarization resistance, R_p, is 38.5%, much higher than that of the cell with PBSCF cathode, consistent with the significant improvement of the performance. The significant reduction in both R_Ω and R_p shows that cathodic polarization current not only improves the physical contact between the cathode and YSZ electrolyte interface, but also the contact between PBSCF and GDC particles within the composite cathode. The R_p is 0.58 and 0.89 Ω cm^2 at 700 and 650 °C, respectively.

The stability of the SOFCs is an important factor in the evaluation of the electrochemical activity of the electrodes. Fig. 4a shows the stability test of the cells with *in situ* assembled PBSCF-GDC composite cathode under a constant current density of 500 mA cm^{-2} at 750 °C. The voltage initially increases from 0.87 to 0.92 V, and stays around 0.92 V for 70 h, showing rather stable performance. However, the cell voltage decreases slightly to 0.88 V with further polarization. The R_Ω remains approximately the same value before and after the 100 h test, as shown in Fig. 4b. The R_p is 0.30 Ω cm^2 after tested for 50 h, very close to the initial value 0.32 Ω cm^2 of the cell before the test, and it increases slightly to 0.42 Ω cm^2 at the end of the test. The increase in polarization resistance is mainly on the low frequencies. The impedance

responses of the cells can be characterized by a small depressed high-frequency arc and a large low-frequency arc, as normally observed for conventional anode supported SOFCs.[18, 19] The high-frequency region is normally dominated by cathode process while the low-frequency region can be mainly contributed to anode process.[20-22] An equivalent circuit with two RQ (R is electrode polarization resistance and Q is the constant phase element) elements in series was used for the EIS analysis and the fitting data are shown in Fig. 4b. The polarization resistance values of both high- and low-frequency arc slightly increase after the long-term polarization, as shown in Fig. 4c. As the low frequency of the cell is primarily related to the impedance of the anode of the cell, the small degradation of the cell with *in situ* assembled PBSCF-GDC cathode is also caused by the deterioration of the Ni-YSZ anode.

3.3 Microstructure and AFM analysis of the interface

Fig. 5 shows the SEM micrographs of the cross-sections of the cell with *in situ* assembled PBSCF-GDC composite cathode after tested at 500 mA cm^{-2} and 750 °C for 100 h. The thickness of composite cathode is ~20 μm and the thickness of the YSZ electrolyte layer is 6.5 μm. The PBSCF-GDC cathode is well adhered to YSZ electrolyte layer, and the composite cathode is characterized by a mixture of large and small particles (Fig. 5b). The morphology and microstructural change at the cathode/electrolyte interfaces before and after the durability test were investigated by AFM, and the results are shown in Fig. 6. The freshly prepared YSZ surface is clean with clear grains and boundaries (Fig. 6a). After polarization at 500 mA cm^{-2} and

750 °C for 100 h, there are large number of contact marks formed on the YSZ electrolyte surface in contact with the *in situ* assembled PBSCF-GDC composite cathode (Fig. 6b-c). The size of the contact marks is in the range of 0.1-1 μm. The contact marks are randomly distributed on the surface of YSZ electrolyte, indicating the formation of such formed contact marks is the result of the polarization under SOFC operation conditions. The height profiles along selected three contact marks are given in Fig. 6e. For an individual particle (green line), the difference in height between the highest and lowest points is 24 nm, much lower than its width of 170 nm, which implies the formation of electrode/electrolyte interface. Some small particles aggregate to form islands. The thickness of the islands marked by red and blue lines is 80 and 180 nm, respectively.

The composition and distribution of elements on the YSZ electrolyte surface of the cells after the stability test were investigated by the TOF-SIMS technique and the results are shown in Figure 7. A 10×10 μm scan area was analyzed with the depth of 160 nm (indicated in the Fig.7a). There are large number of particles embedded in YSZ grains forming good contact between the YSZ electrolyte layer and the cathode layer, consistent with the AFM result in Fig. 6. The element mapping of Zr, Ce, Ba and Sr at the depth of 50 nm are shown in Fig. 7b. Strong signal of Zr is detected on the whole area, while Ce element is also detected on the YSZ electrolyte surface. However, the signals of Ba and Sr are extremely weak as compared to that of Ce, which implies that most of those remained particles on the YSZ surface are GDC particles from the cathode layer. The results indicate that cathodic polarization current

could be beneficial for the interfacial contact between GDC and YSZ electrolyte.

The in situ assembly of PBSCF electrode on YSZ electrolyte and the formation of electrode/electrolyte interface under the influence of cathodic polarization are schematically shown in Fig.8. In this *in situ* assembly route, the cathode powder is directly applied on barrier-layer-free YSZ electrolyte, followed by in situ assembling under operation conditions. The current passage works as a driving force for the contact and interface between the PBSCF and GDC particles, forming passages for ionic and electronic transfer (Fig.8c). More importantly, the interfaces between the YSZ electrolyte and the cathode can be formed electrochemically *in situ* under SOFC operation conditions (Fig. 8d). ??

4 Conclusions

In this study, *in situ* assembling method was used to apply PBSCF double perovskite cathode material directly to Ni-YSZ anode supported YSZ electrolyte based SOFCs. After polarization treatment at 500 mA cm^{-2} and 750 °C for 2 h, electrochemical performance of the cells was remarkably improved. Cathodic polarization reduced the cell ohmic resistance, indicating the formation of electrochemically induced interface. This is confirmed by the AFM examination of the YSZ electrolyte surface in contact with the *in situ* assembled PBSCF-GDC cathodes. In the case of the cell with *in situ* assembled PBSCF-GDC composite cathode, the maximum power density was 1.37 W cm^{-2} at 750 °C. And it shows quite high stability under polarization conditions of 500 $mAcm^{-2}$ and 750 °C for 100 h. The

TOF-SIM analysis reveals that large number of GDC particles were embedded in YSZ grains forming good contact between the electrolyte and cathode layers after polarization. The above results demonstrate that the *in situ* assembly method is an effective approach to directly apply cobaltite-based double perovskite cathodes to YSZ electrolyte based SOFCs.

Acknowledgements

This project is supported by the National Natural Science Foundation of China (project number: 51472099) and the Australian Research Council under the Discovery Project Scheme (project number: DP150102025 & DP150102044). The authors acknowledge the facilities, scientific and technical assistance of the Curtin University Microscopy & Microanalysis Facility, Curtin University.

References

1. S. P. Jiang, *Journal of Materials Science*, 2008, **43**, 6799-6833.

2. E. P. Murray, T. Tsai and S. A. Barnett, *Solid State Ionics*, 1998, **110**, 235-243.

3. Y. Takeda, R. Kanno, M. Noda, Y. Tomida and O. Yamamoto, *J. Electrochem. Soc.*, 1987, **134**, 2656-2661.

4. R. Pelosato, G. Cordaro, D. Stucchi, C. Cristiani and G. Dotelli, *J. Power Sources*, 2015, **298**, 46-67.

5. A. Y. Suntsov, I. A. Leonidov, M. V. Patrakeev and V. L. Kozhevnikov, *Solid State Ionics*, 2015, **274**, 17-23.

6. M. Burriel, J. Pena-Martinez, R. J. Chater, S. Fearn, A. V. Berenov, S. J. Skinner and J. A. Kilner, *Chem Mater*, 2012, **24**, 613-621.

7. S. Choi, S. Yoo, J. Kim, S. Park, A. Jun, S. Sengodan, J. Kim, J. Shin, H. Y. Jeong, Y. Choi, G. Kim and M. Liu, *Scientific Reports*, 2013, **3**, 2426.

8. L. Jiang, T. Wei, R. Zeng, W.-X. Zhang and Y.-H. Huang, *J Power Sources*, 2013, **232**, 279-285.

9. S. Park, S. Choi, J. Shin and G. Kim, *RSC Advances*, 2014, **4**, 1775-1781.

10. Y.-M. Kim, P. Kim-Lohsoontorn and J. Bae, *J Power Sources*, 2010, **195**, 6420-6427.

11. S.-W. Baek, J. Jeong, Y.-M. Kim, J. H. Kim, S. Shin and J. Bae, *Solid State Ionics*, 2011, **192**, 387-393.

12. C. Lee and J. Bae, *J Power Sources*, 2008, **176**, 62-69.

13. I. Villarreal, C. Jacobson, A. Leming, Y. Matus, S. Visco and L. De Jonghe,

Electrochemical and Solid-State Letters, 2003, **6**, A178-A179.

14. S. P. Jiang, *J Electrochem Soc*, 2015, **162**, F1119-F1128.

15. M. Mori, T. Yamamoto, H. Itoh, H. Inaba and H. Tagawa, *J Electrochem Soc*, 1998, **145**, 1374-1381.

16. M. Mori, Y. Hiei, N. M. Sammes and G. A. Tompsett, *J Electrochem Soc*, 2000, **147**, 1295-1302.

17. Q. L. Liu, K. A. Khor, S. H. Chan and X. J. Chen, *J. Power Sources*, 2006, **162**, 1036-1042.

18. Z. Zhan and S. A. Barnett, *Solid State Ionics*, 2005, **176**, 871-879.

19. B. Hua, M. Li, Y.-F. Sun, Y.-Q. Zhang, N. Yan, J. Chen, J. Li, T. Etsell, P. Sarkar and J.-L. Luo, *Journal of Materials Chemistry A*, 2016, **4**, 4603-4609.

20. S. McIntosh, J. M. Vohs and R. J. Gorte, *J. Electrochem. Soc.*, 2003, **150**, A1305-A1312.

21. S. Cho, D. E. Fowler, E. C. Miller, J. S. Cronin, K. R. Poeppelmeier and S. A. Barnett, *Energy & Environmental Science*, 2013, **6**, 1850-1857.

22. K. F. Chen, L. Zhang, N. Ai, S. Zhang, Y. Song, Y. C. Song, Q. Yi, C. Z. Li and S. P. Jiang, *Energy Fuels*, 2016, **30**, 1849-1857.

Figure captions:

1. (a) The XRD pattern of as-prepared PBSCF calcined in air at 1050 °C for 10 h and (b) thermal expansion curve of PBSCF collected in air at temperatures ranging from 200 to 900 °C.
2. (a) Polarization performance and (b) open circuit EIS of the cell with in situ assembled PBSCF cathode, measured at 750 °C before and after polarization at 500 mA cm^{-2} for 2 h. The performance of a full cell prepared by conventional method with a GDC buffer layer is illustrated for comparison.
3. (a) Polarization performance and (b) open circuit EIS of the cell with in situ assembled PBSCF-GDC composite cathode, measured at temperatures ranging from 650 to 750 °C after polarization at 500 mA cm^{-2} and 750 °C for 2 h. The initial performance at 750 °C before polarization treatment was also recorded for comparison.
4. (a) Performance stability of the cell with PBSCF-GDC composite cathode at 500 mA cm^{-2} and 750 °C; and (b) open circuit impedance curves and (c) corresponding fitting data of the cell.
5. SEM micrographs of cross sections of (a) the full cell and (b) PBSCF-GDC composite cathode after the stability test.
6. AFM micrographs of (a) a blank YSZ electrolyte surface for comparison and (b-c) YSZ electrolyte surface in contact with *in situ* assembled PBSCF-GDC composite cathode after the cell stability test. (d) Height image of the area shown in (c). (e) The height profile along the line indicated in (d).

7. (a) SEM images of the YSZ electrolyte surface in contact with *in situ* assembled PBSCF-GDC composite cathode after the cell stability test. (b) TOF-SIMS element representations from a 10×10 μm scan area indicated in (a) at the depth of 50 nm.
8. Scheme of the in situ assembly process.

Figure 1.

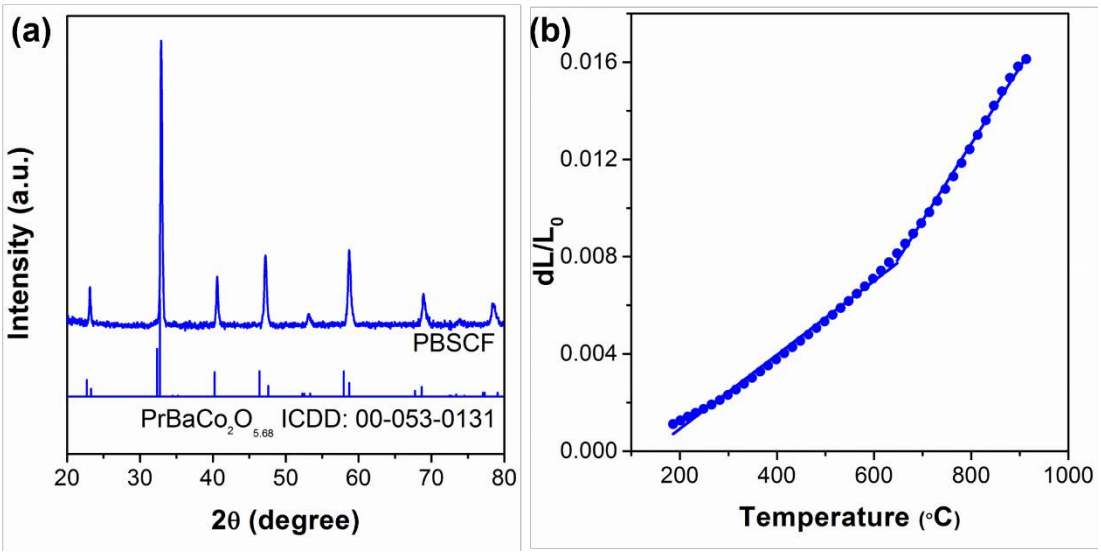
(a)
Intensity (a.u.)
PBSCF
PrBaCo2O5.68 ICDD: 00-053-0131
20
30
40
50
60
70
80
2θ (degree)
(b)
0.016
0.012
0.008
0.004
0.000
dL/L0
200
400
600
800
1000
Temperature (°C)

Figure 2.

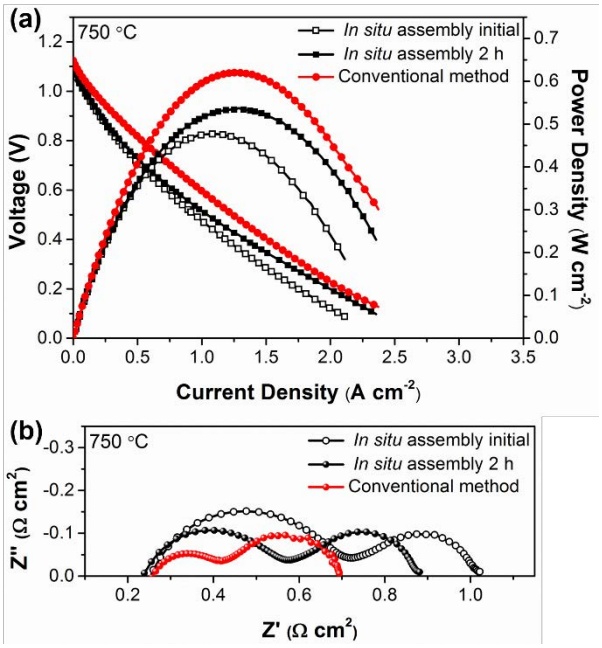
(a)
750 °C
In situ assembly initial
In situ assembly 2 h
Conventional method
Voltage (V)
Power Density (W cm-2)
Current Density (A cm-2)
(b)
750 °C
In situ assembly initial
In situ assembly 2 h
Conventional method
Z'' (Ω cm2)
Z' (Ω cm2)

Figure 3.

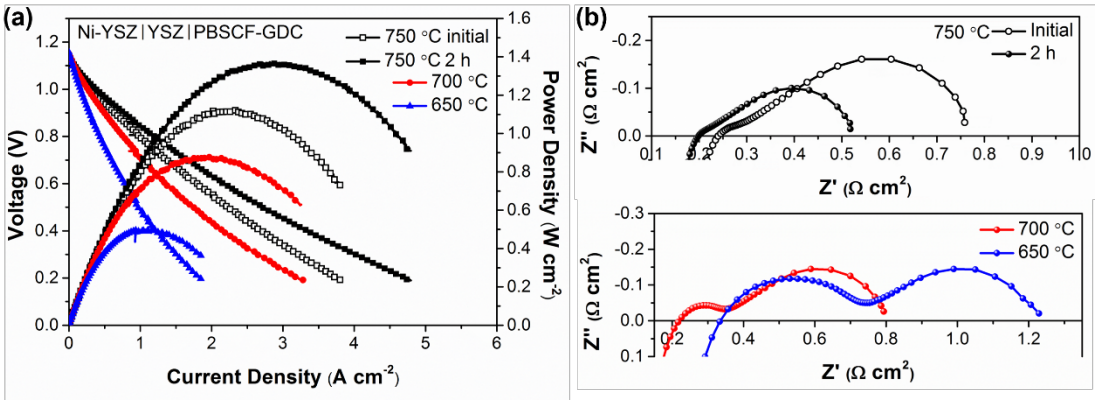
(a)
Ni-YSZ|YSZ|PBSCF-GDC
750 °C initial
750 °C 2 h
700 °C
650 °C
Voltage (V)
Power Density (W cm-2)
Current Density (A cm-2)
(b)
750 °C
Initial
2 h
Z'' (Ω cm2)
Z' (Ω cm2)
700 °C
650 °C

Figure 4.

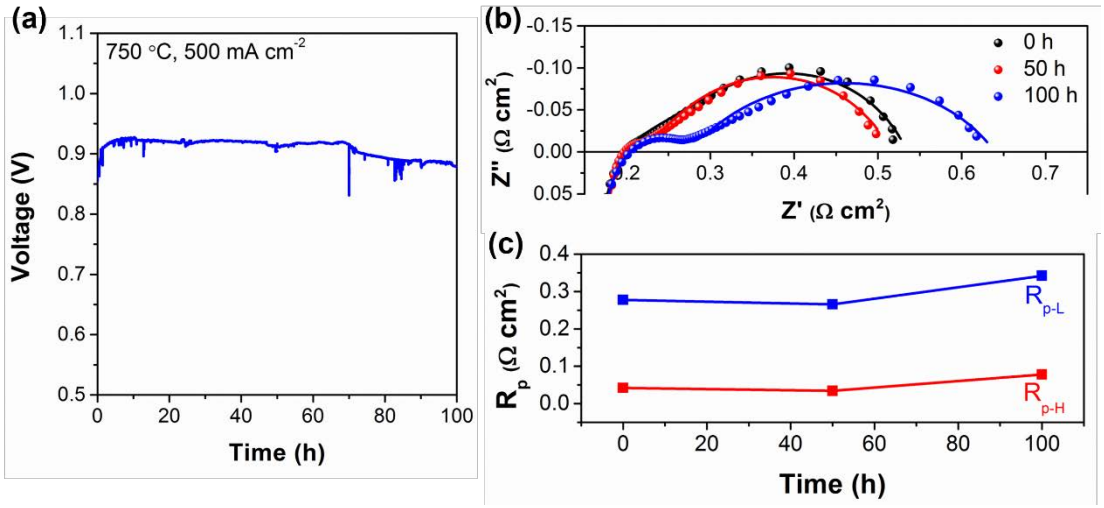
(a)
750 °C, 500 mA cm-2
Voltage (V)
Time (h)
(b)
0 h
50 h
100 h
Z'' (Ω cm2)
Z' (Ω cm2)
(c)
Rp (Ω cm2)
Rp-L
Rp-H
Time (h)

Figure 5.

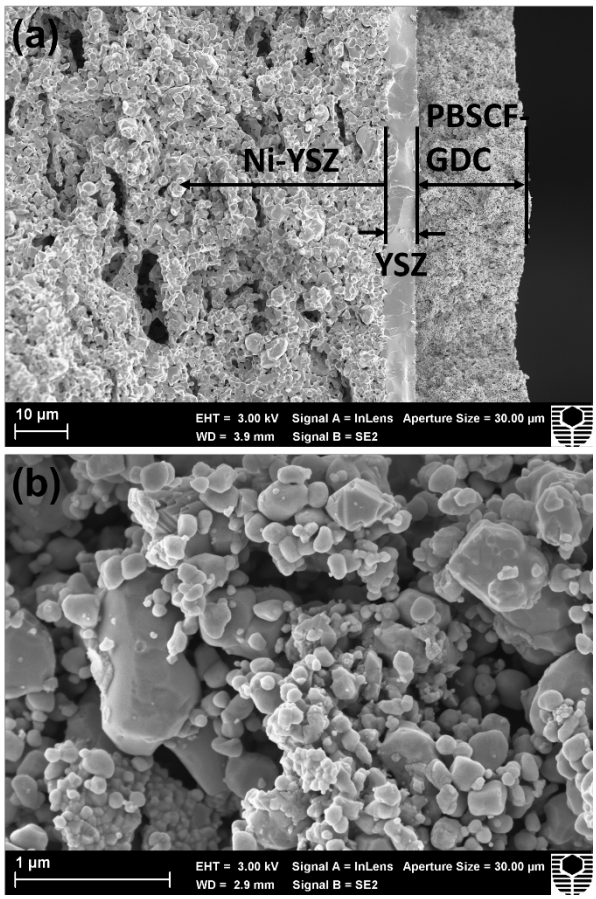
(a)
Ni-YSZ
PBSCF
GDC
YSZ
10 µm
EHT = 3.00 kV
WD = 3.9 mm
Signal A = InLens
Signal B = SE2
Aperture Size = 30.00 µm
(b)
1 µm
EHT = 3.00 kV
WD = 2.9 mm
Signal A = InLens
Signal B = SE2
Aperture Size = 30.00 µm

Figure 6.

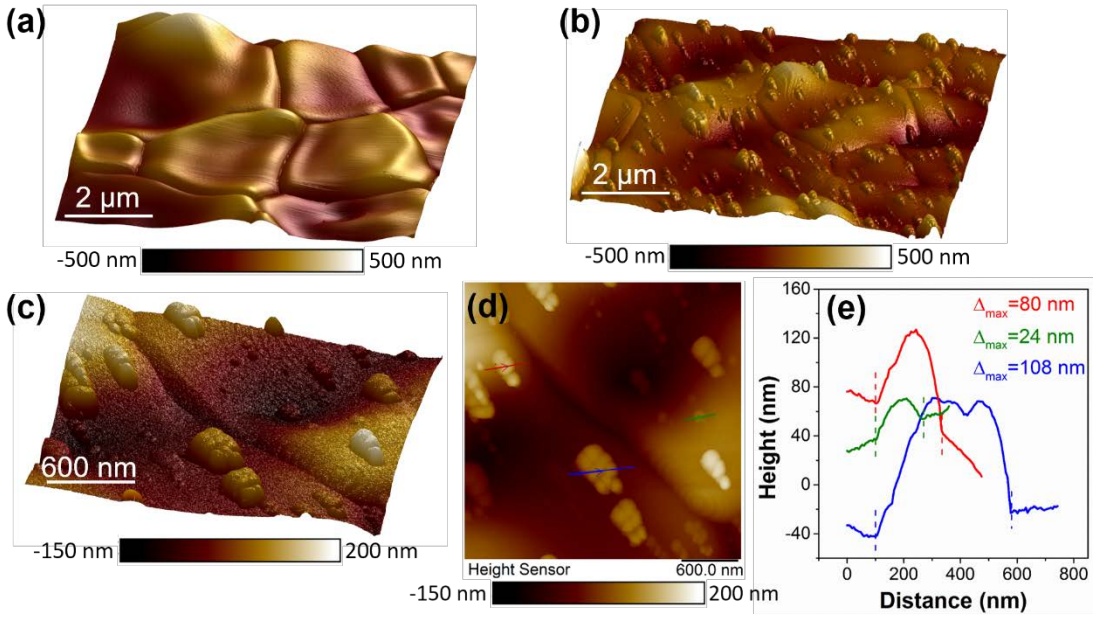
(a)
2 μm
-500 nm
500 nm
(b)
2 μm
-500 nm
500 nm
(c)
600 nm
-150 nm
200 nm
(d)
Height Sensor
600.0 nm
-150 nm
200 nm
(e)
Δmax=80 nm
Δmax=24 nm
Δmax=108 nm
Height (nm)
160
120
80
40
0
-40
0
200
400
600
800
Distance (nm)

Figure 7.

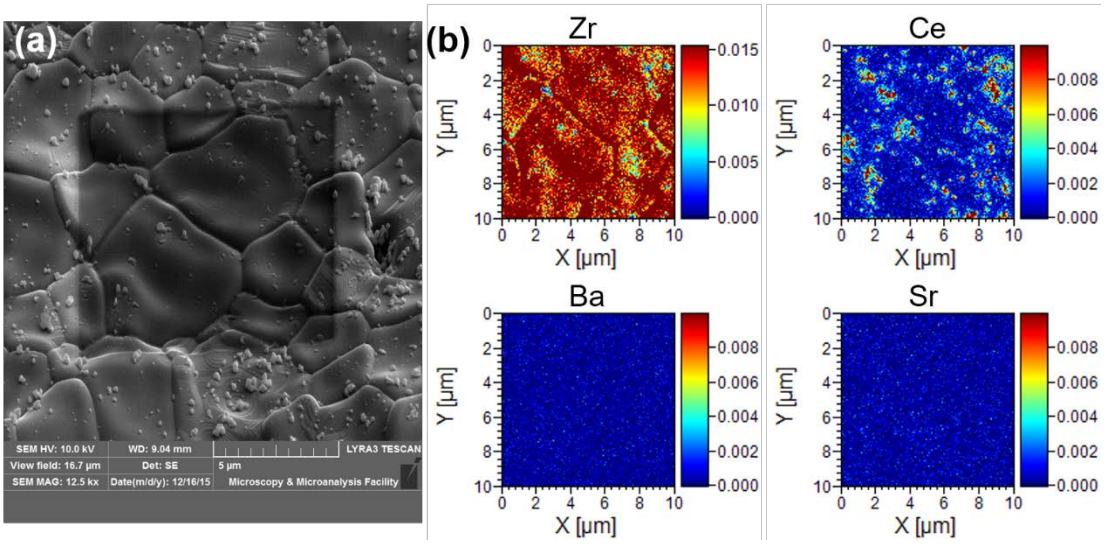
(a)
SEM HV: 10.0 kV
WD: 9.04 mm
LYRA3 TESCAN
View field: 16.7 µm
Det: SE
5 µm
SEM MAG: 12.5 kx
Date(m/d/y): 12/16/15
Microscopy & Microanalysis Facility
(b)
Zr
Ce
Ba
Sr
Y [µm]
X [µm]

Figure 8.

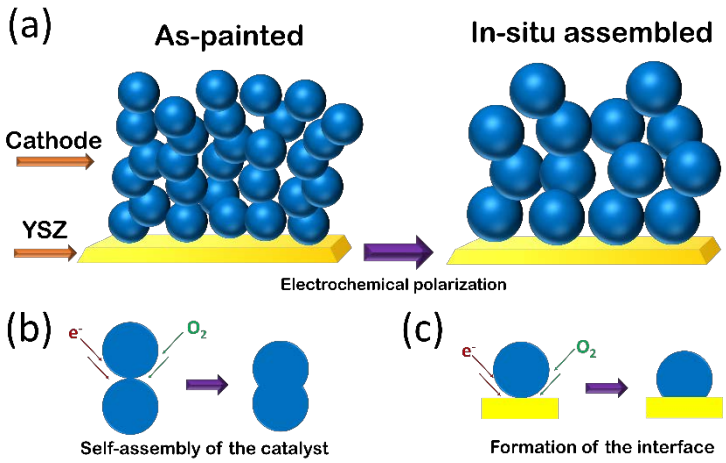
(a)
As-painted
In-situ assembled
Cathode
YSZ
Electrochemical polarization
(b)
e-
O2
Self-assembly of the catalyst
(c)
e-
O2
Formation of the interface